Perraki, Georgia; Roncoli, Claudio; Papamichail, Ioannis; Papageorgiou, Markos

Evaluation of a model predictive control framework for motorway traffic involving conventional and automated vehicles

Published in:
Transportation Research Part C: Emerging Technologies

DOI:
10.1016/j.trc.2018.05.002

Published: 01/07/2018

Document Version
Peer reviewed version

Evaluation of a model predictive control framework for motorway traffic involving conventional and automated vehicles

Georgia Perraki[a,*], Claudio Roncoli[b], Ioannis Papamichail[a], Markos Papageorgiou[a]

[a] *Dynamic Systems and Simulation Laboratory, Technical University of Crete, Chania 73100 Greece*

[b] *Department of Built Environment, School of Engineering, Aalto University, Espoo 02150 Finland*

[*] Corresponding author

Email addresses: gperraki@isc.tuc.gr (Georgia Perraki), claudio.roncoli@aalto.fi (Claudio Roncoli), ipapa@dssl.tuc.gr (Ioannis Papamichail), markos@dssl.tuc.gr (Markos Papageorgiou)

Preprint submitted to Transportation Research Part C *April 14, 2018*

Abstract

A Model Predictive Control (MPC) strategy for motorway traffic management, which takes into account both conventional control measures and control actions executed by vehicles equipped with Vehicle Automation and Communication Systems (VACS), is presented and evaluated using microscopic traffic simulation. A stretch of the motorway A20, which connects Rotterdam to Gouda in the Netherlands, is taken as a realistic test bed. In order to ensure the reliability of the application results, extensive speed and flow measurements, collected from the field, are used to calibrate the site's microscopic traffic simulation model. The efficiency of the MPC framework, applied to this real sizable and complex network under realistic traffic conditions, is examined for different traffic conditions and different penetration rates of equipped vehicles. The adequacy of the control application when only VACS equipped vehicles are used as actuators, is also considered, and the related findings underline the significance of conventional control measures during a transition period or in case of increased future demand.

Keywords: Motorway traffic control, Model predictive control, Connected and autonomous vehicles, Microscopic traffic simulation, Aimsun

1. Introduction

Traffic congestion is associated with a variety of problems that modern societies face. Increased travel times, infrastructure degradation, and excessive environmental pollution are some of the negative consequences of traffic congestion, rendering the need for efficient traffic management stronger than ever. In this context, the development of various types of Vehicle Automation and Communication Systems (VACS) during the last decade may prove beneficial, not only for the individual driver safety and convenience, but also for their employment as important tools of innovative traffic management approaches (Diakaki et al., 2015). It should be noted however that the mere existence of VACS is no guarantee for improved traffic flow efficiency, and, in fact, VACS may even lead to deterioration of the traffic conditions if their introduction is not accompanied by proper traffic management measures. Thus, the development of traffic control strategies that exploit VACS efficiently has been the subject of several works.

In some early works on the subject, Varaiya (1993) proposed the use of intelligent devices in Automated Highway Systems (AHS), where it was assumed that platoons of fully automated vehicles may travel in specifically designed motorways. This complex system was suggested to be controlled through a three-layer control structure, where the decentralized traffic flow control tasks are implemented via roadside and vehicle computers (Rao and Varaiya, 1994). The possibility of semi-automated or fully automated driving, leading to lane assignment problems for AHS, is considered by Kim et al. (2008). Baskar et al. (2011), provide an in-depth analysis of the traffic control measures for Intelligent Vehicle Highway Systems (IVHS) and give an

overview of developed control schemes that combine roadside controllers and automated platoons.

Besides the decentralized control approaches for AHS, a lot of research has been conducted on the impact of the currently existing driver assistance systems on the motorway traffic flow conditions (see e.g., Rao and Varaiya 1993; Vander Werf et al. 2002; Davis 2004). Kesting et al. (2007) proposed an Adaptive Cruise Control (ACC)-based in-vehicle strategy, capable to overcome the potential negative impact of the driver assistance system on the traffic conditions and to improve the overall traffic situation on the motorway. The experiments conducted by Shladover et al. (2012), using real equipped vehicles, have shown that, in case sufficient amount of vehicles equipped with cooperative ACC, the highway capacity can be increased, in contrast to the case of automated ACC systems, which resulted in minor impact on the capacity values. Wang et al. (2014a) presented a control framework whereby vehicles equipped with Advanced Driver Assistance Systems (ADAS) are enabled to set their acceleration based on the prediction of the neighboring vehicles behavior over a time horizon. This control scheme was modified by Wang et al. (2014b), where the possibility of synergistic control actions and information exchange between vehicles is considered with the introduction of cooperative ADAS. In the work by Spiliopoulou et al. (2017), an ACC-based control scheme is presented where the settings of the ACC system are adjusted based on the traffic conditions of specific motorway sections. This traffic control strategy was tested using microscopic traffic simulations and resulted in significant improvements of the average vehicle delay as well as of the fuel consumption rates.

Although the main research interest lies in the exploitation of ADAS systems for longitudinal flow control, some recent studies have emphasized the advantages of cooperative lane-changing with the use of Vehicle-to-Vehicle (V2V) communication systems. Ammoun et al. (2007) presented a lane-changing assisting system, capable to predict the trajectory of the vehicle and to examine risks associated with potential lane change maneuvers based on the information received from the neighboring vehicles. The presented model was validated with real data from tests involving an intelligent vehicle and showed sufficient performance. More recently, a decentralized control framework for cooperative lane-changing was proposed by Nie et al. (2016), where it is considered that connected automated vehicles take lane-changing decisions with the aim of improving the traffic situation in the motorway. The lane-changing decision depends on a state prediction module, which aims at predicting the state of the vehicles related to the automated vehicle in the next time intervals, and a candidate decision generation module, where the candidate decisions of each vehicle are produced based on information received by the neighboring vehicles.

This paper is an extension of Perraki et al. (2017) and adopts the Model Predictive Control (MPC) strategy proposed by Roncoli et al. (2016a) to evaluate various interesting aspects of innovative and conventional traffic control measures for a complex real network in a realistic simulation environment. Specifically, the applicability and effectiveness of the strategy is tested for various combinations of control measures and different penetration rates of equipped vehicles using a complex real infrastructure which is simulated by use of the Aimsun (Transport Simulation Systems, 2014) microscopic traffic

simulator, after careful calibration and validation on the basis of real traffic data. The model is fed with real measured demands, creating a realistic and sizable virtual test-bed for comprehensive and multi-faceted evaluation. The core of the control strategy is the convex optimization problem proposed by Roncoli et al. (2015b), which includes, as decision variables, actions enabled with the aid of VACS as well as conventional traffic control measures. The optimal control problem formulation is based on a piecewise-linear macroscopic traffic flow model developed by Roncoli et al. (2015a), which is however extended in the present work with the introduction of a piecewise-linear fundamental diagram in order to capture under-critical conditions more efficiently. Moreover, while in the earlier work of Roncoli et al. (2016a) the primary control scheme had been preliminarily tested using microscopic traffic simulation for a limited hypothetical infrastructure, this paper explores the efficiency of the strategy for a challenging and sizable real-life network with the no-control case being the real reference case for the traffic conditions in the motorway. In addition, we examine the case where the conventional control measures are deactivated from the control application, so as to enable conclusions to be drawn regarding the adequacy of the control actions which are exclusively performed by VACS-equipped vehicles.

The rest of the paper is organized as follows. Section 2 gives a brief overview of the optimal control problem and the employed MPC scheme. In Section 3, the case study network is described, along with the behavioral models and the dynamic scenario used in the microscopic simulation. Then, the calibration process is presented, and the simulated speeds are compared to the real measured speeds in order to demonstrate that the microscopic

simulation is capable of replicating reality. In Section 4, the setup of the MPC strategy is specified, and the control strategy is applied to the calibrated model for different penetration rates of equipped vehicles. Subsequently, the outcome of a modified control scheme, that considers only the control actions executed by VACS-equipped vehicles, is investigated. Finally, Section 5 summarizes the main findings of the work.

2. Model Predictive Control for integrated and coordinated motorway traffic control

2.1. Control framework

Several approaches have been presented in the literature for the problem of optimal coordinated and integrated motorway traffic control (see, e.g., Kotsialos et al. 2002, Hegyi et al. 2005a). The application of these approaches cannot be effectuated in an open-loop manner due to inevitable discrepancies from reality of the employed models and external variable (e.g. demand) prediction. Such discrepancies are mitigated by use of an MPC framework , whereby the optimal control problem is solved repeatedly in real time with updated initial traffic state and demand predictions; while only a small initial part of the computed optimal control trajectories are actually applied, before the next updated optimization. Each optimization features a finite time horizon, which is "rolled" with subsequent optimal control computations, hence the synonym "rolling horizon control" for MPC. Some experiments that highlight the efficiency of MPC for the motorway traffic control problem can be found in Hegyi et al. (2005a), van den Berg et al. (2007), Baskar et al. (2012).

Within such an MPC framework, we employ an optimal control problem, which takes into account the possible use of VACS as sensors and as actuators while operating in closed loop. The full motorway traffic control framework, which is developed by Roncoli et al. (2016a), is designed to operate as a multi-layer application. The necessary traffic data, retrieved either from fixed sensors or from equipped vehicles, is processed by an adaptation and prediction layer with the purpose of estimating the current traffic state and predicting the sort-term traffic demand. Subsequently, the outcome of this layer is used in order to solve the optimal control problem within the optimization layer and, finally, the numerical solution derived from the optimization problem is converted to actually applicable control actions in the application layer. It is worth mentioning that multi-layer control structures have been employed for several control applications, including traffic control problems (see e.g. Papageorgiou 1984, Papamichail et al. 2010, Wang et al. 2016), each time of course with varying specific contents within each control layer.

2.2. Optimal control problem

The control strategy employs a piecewise linear macroscopic traffic flow model that was first introduced by Roncoli et al. (2015a). Herein, this model is further developed with the introduction of a new type of fundamental diagram. Consequently, the extended model is used and tested in the same optimal control framework that was first described by Roncoli et al. (2015b). For the sake of completeness, the basic concepts of the control problem formulation are presented below, while the reader may refer to the aforementioned publications for more details.

The multi-lane motorway is subdivided into $i = 1, ..., I$ segments and $j = 1, ..., J$ lanes. Each segment-lane entity is denoted as a cell, indexed by (i, j). The control measures that are considered in the proposed framework are the following:

- Ramp Metering (RM): It aims at controlling the inflow from the on-ramps to the motorway mainstream. For RM application, conventional traffic lights are commonly employed to limit the entering flow via proper specification of red and green phases based on the desired ramp outflow resulted from the optimal control problem. Several approaches for local and coordinated ramp metering based on conventional measures can be found in literature (Kotsialos and Papageorgiou 2004; Papamichail et al. 2010; Davarynejad et al. 2011), while many studies have highlighted the advantages of integrated control involving RM and Variable Speed Limits (VSL) measures (Hegyi et al. 2005a; Abdel-Aty and Dhindsa 2007; Papamichail et al. 2008; Carlson et al. 2010; Iordanidou et al. 2017). It should be noted however, that with the increased number of vehicles equipped with VACS, direct commands sent via Vehicle-to-Infrastructure (V2I) communication systems may also be used for the execution of the ramp metering actions.

- Mainstream Traffic Flow Control (MTFC) via VSL: The use of VSL in order to regulate the motorway mainstream flow has been proposed in various conventional traffic control approaches (Breton et al. (2002); Hegyi et al. (2005b); Lee et al. (2006); Carlson et al. (2011); Yang et al. (2013); Iordanidou et al. (2015)). In cases of conventional traffic, the speed limits are indicated with the use of Variable Message Signs

(VMS), located on gantries, which display the same speed limit for all lanes at a fixed space resolution determined by the gantry positions. However, the emerging presence of vehicles equipped with VACS can advance the application of VSL, since the drivers may directly receive specific speed limits according to their current location and lane. Moreover, in cases of automated vehicles, the potential of direct application of the VSL in the driving system without the driver's intervention is expected to further ameliorate the control actions execution. It should be noted that some legal issues may arise on the perspective of automated vehicles receiving different speed limits than those perceived by conventional vehicle drivers while driving on motorways, which could be addressed via additional presence of VSL gantries in periods of still low penetration of VACS. In the presented framework, it is assumed that all the VACS-equipped vehicles traveling in the network can receive and apply a specific speed limit. The value of the speed limit is delivered by the control strategy for each cell, and it is expected that, for a sufficient penetration of equipped vehicles, this will be sufficient to impose the speed limit to non-equipped vehicles as well; hence, no VMS-gantries would be needed.

- Lane Changing Control (LCC): This control action, which is not applicable in conventional traffic, may be implemented by sending lane-changing advise to an appropriate number of selected VACS-equipped vehicles in each cell. The problem of optimal lane-assignment with the purpose of improving safety and increasing traffic throughput in motorways has been addressed in some works in the past (Varaiya 1993;

Dao et al. 2007, 2008). More recently, Roncoli et al. (2016b, 2017) presented a feedback control scheme for lane-changing control at bottleneck locations, where vehicles equipped with VACS are capable of receiving and executing lane-changing orders. It should be noted that future cooperative lane-changing capabilities of vehicles equipped with V2V communication systems may further enhance the application of the LCC actions.

For flexibility, it is supposed that each of the aforementioned control actions is updated according to its specific control time step which may be specified based on human-factors and other operational requirements. The control time steps are assumed to be integer multiples of the traffic flow model time step. Specifically, we denote by T the model time step for an optimization horizon K indexed by $k = 0, 1, 2, .., K$, where the simulation time is $t = kT$. The motorway is discretized in space with the definition of cells (i, j), and each motorway cell is characterized by the following variables:

- Density $\rho_{i,j}(k)$ [veh/km]: The number of vehicles in cell (i, j), at time step k, divided by the segment length L_i.
- On-ramp queue $w_{i,j}(k)$ [veh]: The number of vehicles queuing at the step k at the on-ramp (if any) attached to the motorway at cell (i, j).
- On-ramp flow $r_{i,j}(k^R)$ [veh/h]: The traffic volume entering from the on-ramp (if any) located at cell (i, j) during the time interval $(k^R, k^R + 1]$,

where $k^R = \lceil \frac{kT}{T^R} \rceil$ [1] and T^R is the control step for RM. This is a control variable that reflects the RM actions.

- Longitudinal flow $q_{i,j}(k^Q)$ [veh/h]: The traffic volume leaving segment i and entering segment $i+1$, remaining in lane j, during time interval $(k^Q, k^Q+1]$, where $k^Q = \lceil \frac{kT}{T^Q} \rceil$ and T^Q is the control step for MTFC. This is the control variable regarding MTFC actions.

- Lateral flow $f_{i,j,\bar{j}}(k^F)$ [veh/h]: The traffic volume moving from lane j to lane $\bar{j} = j \pm 1$, remaining in the same segment, during time interval $(k^F, k^F+1]$, where $k^F = \lceil \frac{kT}{T^F} \rceil$ and T^F is the control step for LCC. This is a control variable that reflects the LCC actions.

The following conservation law equation describes the dynamics of densities $\rho_{i,j}(k)$ [veh/km] for each cell (i,j), where the off-ramp flow is determined based on the time-varying turning rates $\gamma_{i,j}(k)$:

$$\begin{aligned}\rho_{i,j}(k+1) = \quad & \rho_{i,j}(k) + \tfrac{T}{L_i}[q_{i-1,j}(k^Q) + r_{i,j}(k^R) - q_{i,j}(k^Q) - \gamma_{i,j}(k)\textstyle\sum_{j=1}^{J} q_{i,j}(k^Q) \\ & + f_{i,j+1,j}(k^F) + f_{i,j-1,j}(k^F) - f_{i,j,j-1}(k^F) - f_{i,j,j+1}(k^F)];\end{aligned} \tag{1}$$

while the dynamics of queues formed at the on-ramps due to RM actions, with $d_{i,j}(k)$ being the external (known) demand, is:

$$w_{i,j}(k+1) = w_{i,j}(k) + T[d_{i,j}(k) - r_{i,j}(k^R)]. \tag{2}$$

The modeling approach for longitudinal flows, proposed and tested in (Roncoli et al., 2015a), is based on the piecewise-linear fundamental diagram

[1] The ceiling function $y = \lceil x \rceil$ is used here, where y is the smallest integer greater than or equal x.

illustrated in Figure 1. The fundamental diagram consists of a demand and a supply part which determine the flow according to the upstream and downstream density, respectively. This traffic flow model extends the well known Godunov-discretized LWR (Lighthill and Whitham, 1955) model, with a modification in the demand function in order to include the possibility to reflect the capacity drop phenomenon, which plays a critical role in designing and assessing traffic control strategies. In particular, the capacity drop is modelled with the introduction of a linear function in the demand part that decreases according to the slope w^D in case the density $\rho_{i,j}(k)$ in the upstream cell exceeds the critical density $\rho_{i,j}^{cr}$. The flow that is allowed to leave a completely congested cell i.e. $\rho_{i,j}(k) = \rho_{i,j}^{jam}$ (where $\rho_{i,j}^{jam}$ is the maximum admissible density) is denoted as $q_{i,j}^{jam}$, while in the conventional CTM (Daganzo, 1994), where the capacity drop is not taken into account, this is equal to the capacity flow $q_{i,j}^{max}$. Finally, a new approach to the design of the fundamental diagram for undercritical densities is introduced and employed in the present study. Specifically, the left-hand side of the demand part of the fundamental diagram is modelled as a piecewise linear increasing function, composed by two linear functions, instead of a single linear function, which leads to more realistic representation of undercritical traffic speed behavior (Kontorinaki et al., 2017). Specifically, this approach leads to a speed value (υ^{free}) for undercritical situations, where density does not exceed a threshold density value $\rho_{i,j}^{a}$ ($\rho_{i,j}(k) < \rho_{i,j}^{a}$); and another, lower speed value while approaching the critical density ($\rho_{i,j}^{a} \leq \rho_{i,j}(k) < \rho_{i,j}^{cr}$).

The linear inequalities derived from the utilized piecewise linear fundamental diagram are used to constrain the longitudinal flows which are control

variables of the optimization problem. Hence, inequalities (3), (4) and (5) represent the bounds based on the demand part of the fundamental diagram; while inequalities (6) and (7) represent the bounds based on the supply part of the proposed fundamental diagram.

$$q_{i,j}(k) \leq v_{i,j}^{free} \rho_{i,j}(k) \tag{3}$$

$$q_{i,j}(k) \leq \frac{v_{i,j}^{free} \rho_{i,j}^{a} - q_{i,j}^{max}}{\rho_{i,j}^{a} - \rho_{i,j}^{cr}} \rho_{i,j}(k) + \frac{q_{i,j}^{max} - v_{i,j}^{free} \rho_{i,j}^{cr}}{\rho_{i,j}^{a} - \rho_{i,j}^{cr}} \rho_{i,j}^{a} \tag{4}$$

$$q_{i,j}(k) \leq -\frac{q_{i,j}^{max} - q_{i,j}^{jam}}{\rho_{i,j}^{jam} - \rho_{i,j}^{cr}} \rho_{i,j}(k) + \frac{q_{i,j}^{max} \rho_{i,j}^{jam} - q_{i,j}^{jam} \rho_{i,j}^{cr}}{\rho_{i,j}^{jam} - \rho_{i,j}^{cr}} \tag{5}$$

$$q_{i,j}(k) \leq q_{i+1,j}^{max} \tag{6}$$

$$q_{i,j}(k) \leq -\frac{q_{i+1,j}^{max}}{\rho_{i+1,j}^{jam} - \rho_{i+1,j}^{cr}} \rho_{i+1,j}(k) + \frac{q_{i+1,j}^{max} \rho_{i+1,j}^{jam}}{\rho_{i+1,j}^{jam} - \rho_{i+1,j}^{cr}} \tag{7}$$

Inequality (8) represents the upper-bound for lateral flows, determined by the number of vehicles in the current cell, while inequality (9) is an upper bound considering the available space in the cell that is receiving the lateral flow. Finally, the lateral flows are constrained based on inequality (10) in order to strictly limit lateral movements and to avoid unrealistic values that cannot be materialized in real traffic.

$$[f_{i,j,j-1}(k^F) + f_{i,j,j+1}(k^F)] \leq \frac{L_i}{T} \rho_{i,j}(k) \tag{8}$$

$$[f_{i,j-1,j}(k^F) + f_{i,j+1,j}(k^F)] \leq \frac{L_i}{T} [\rho_{i,j}^{jam} - \rho_{i,j}(k)] \tag{9}$$

$$\begin{aligned} f_{i,j,j-1}(k^F) &\leq f^{max} \\ f_{i,j,j+1}(k^F) &\leq f^{max} \end{aligned} \tag{10}$$

Fixed upper bounds are also considered for the on-ramp queues and flows, i.e. $w_{i,j}(k) \leq w_{i,j}^{max}$, $r_{i,j}(k^R) \leq r_{i,j}^{max}$, as well as for the off-ramp flows

$\gamma_{i,j}(k) \sum_{j=1}^{J} q_{i,j}(k^Q) \leq q_{i,j}^{off,max}$. Finally, non-negativity constraints are specified for all the problem variables.

The optimization problem is formalized as a convex Quadratic Program (QP), characterized by a convex quadratic cost function subject to linear constraints (1)-(10). The cost function $J = J_{\text{TTS}} + J_{\text{Penalty}}$, is composed by two parts; the first part represents the Total Time Spent (TTS) and the second part contains a set of penalty terms. The most important term to be minimized is the TTS which accounts for the overall time vehicles spend while traveling in the network and queuing at the on-ramps, and is given by:

$$J_{\text{TTS}} = T \sum_{k=1}^{K} \sum_{i=1}^{I} \sum_{j=1}^{J} \left[L_i \rho_{i,j}(k) + w_{i,j}(k) \right]. \tag{11}$$

The second part of the cost function, J_{Penalty}, consists of a set of weighted penalty terms. In particular, it includes a linear term that aims at penalizing lateral flows; and several quadratic penalty terms in order to reduce respective time variations of RM and LCC control variables, as well as to reduce time and space fluctuations of the speed values (approximated via appropriate linearised expressions). Appropriate weight coefficients are utilized for each penalty term in order to reflect the respective control priorities. In particular, the weights related to lateral flows can be defined based on the infrastructural characteristics of the network; e.g. drivers approaching a lane-drop or an on-ramp merge may be encouraged to change lane in advance by setting a lower weight in the respective penalization term.

2.3. Design and implementation of the control strategy

As mentioned in Section 2.1, the case study control framework is designed to operate as a multi-layer application. Figure 2 illustrates the connection be-

tween the different components of the control scheme including the exchange of information among the different layers of the control structure.

The collected field data is initially filtered, aggregated and processed by the adaptation and prediction layer so as to produce the required input for the optimization layer. In particular, this layer comprises the critical task of demand prediction, which is a key component of the MPC, whose efficiency depends on the proper forecast of the demand expected during the optimization horizon. Moreover, all the processes required for the real-time traffic state knowledge (to be used as the initial state for the optimization problem) are carried out by this layer as well. The advent of VACS is expected to offer significant capabilities regarding the availability of data, which with conventional vehicles is mainly obtained from road-side traffic sensors at specific locations of the motorway. Note that this could call for a traffic state estimation algorithm, like the one developed by Bekiaris-Liberis et al. (2016), which has been tested by Fountoulakis et al. (2017) using microscopic traffic simulations and extended by Papadopoulou et al. (2018) and Bekiaris-Liberis et al. (2017) to account for multi-lane motorways.

Subsequently, the predicted demand $d_{i,j}(k)$, as well as the traffic state variables $\rho_{i,j}(k)$ and $w_{i,j}(k)$ are used to feed the optimization layer where the optimal control problem presented in Section 2.2 is solved periodically at the predefined control intervals. The outcome of the optimization layer consists of the numerical solution of the optimal control problem which has to be translated to actual control actions to be applied in the motorway system. This task is performed by the application layer which includes procedures for converting the macroscopic control variables $q_{i,j}(k^Q)$, $r_{i,j}(k^R)$ and $f_{i,j,\bar{j}}(k^F)$

to a set of control tasks.

The application of RM actions is performed using ordinary traffic signals at on-ramps, via appropriate green and red phases, which are specified based on the optimal ramp outflows $r_{i,j}(k^R)$ (see Papageorgiou and Papamichail 2008). Alternatively, in presence of VACS, the same impact can be obtained providing the commands directly through an in-car information system.

The optimal longitudinal flows $q_{i,j}(k^Q)$ resulted from the optimization layer are implemented with the employment of proper VSL which are imposed by VACS-equipped vehicles according to their current position (cell) on the motorway. Recall that, the longitudinal flows are constrained within the optimization problem based on linear functions that depend on the current densities, which are updated every model time step; therefore, a control step for the MTFC that includes more than one model steps, would result in excessive constraining of the longitudinal flows. For that reason, a control step that is equal to the macroscopic model step should be initially chosen for the MTFC actions. Eventually, in order to avoid too frequent VSL changes and to apply all the control actions simultaneously, the computed optimal flow values may be averaged according to the desired control application step.

The implementation of LCC actions is more complex. In the present work, it is considered that each VACS-equipped vehicle computes the available gaps on the left and right lanes. The optimal lateral flows, $f_{i,j,\bar{j}}(k^F)$ obtained from the optimization problem at each control step and for each cell, are converted into time-intervals between two consecutive lane-changes. At the end of each determined time-interval, a lane-change command is sent to the vehicle characterized by the largest gap with respect to the neighboring vehicles in

the target lane, which implies that it is the vehicle that will produce the least negative impact on traffic flow while changing lane.

More specific details regarding the configuration and utilized procedures in each layer for the specific case study assessment are provided in Section 4.1.

3. Application site and microscopic traffic simulation model

3.1. Motorway description

In order to test the effectiveness of the aforementioned traffic management strategy, a real motorway stretch is selected as a case study. The considered stretch is part of the motorway A20 in the Netherlands, which connects Rotterdam to Gouda and contains two pairs of on-ramps and off-ramps. The stretch is about 9.3 km in length and is composed by 3 lanes until its 3.6 km, where the leftmost lane drops. Its complex infrastructure features make this road section an intriguing and challenging case for the evaluation of the proposed traffic control scheme, while the real data retrieved from relatively dense detectors provide a good overview of the real traffic conditions. This real data collected from the case study motorway has been also used by Schakel and van Arem (2014).

3.2. Microscopic simulation configuration

Although some automated and connected vehicle technologies are already available, the appearance of a sufficient number of VACS-equipped vehicles is not expected within the next few years. Therefore, the assessment of innovative control schemes, as the one presented in Section 2, which consider

equipped vehicles that perform the assigned control tasks, is only possible via application in a microscopic simulation environment.

The microscopic traffic simulator Aimsun is employed for the purposes of this work, while its microSDK tool is used in order to overwrite the default vehicle behavioral models. The default car-following model used for the longitudinal movement of vehicles in Aimsun, is based on the model developed by Gipps (1981). This model, however, cannot always reproduce capacity drop phenomena in critical regimes (Wang et al., 2005) and, for this reason, it has been replaced with the Intelligent Driver Model (IDM) car-following model (Treiber et al., 2000). The IDM can reflect significant aspects of the traffic flow dynamics and although the tests conducted by (Milanés and Shladover, 2014) revealed some weaknesses of the model regarding the response to speed changes, the fact that it exhibits crash-free vehicle behavior and smooth adaptation to new traffic conditions (Kesting et al., 2010) makes it a reasonable choice for simulating ACC vehicles.

The default lane-changing model utilized by the Aimsun microscopic simulator is the Gipps lane-changing model (Gipps, 1986). The main limitation of this model is that it cannot capture realistically the merging behavior in a critical flow regime (Chevallier and Leclercq, 2009) and therefore it was complemented at merging network locations with some heuristic rules that were firstly introduced by Roncoli et al. (2016a). These heuristic rules consist of a set of inequality conditions considering the vehicle's current state, the neighboring traffic conditions and some threshold values. In particular, linear functions of the vehicle's current position determine the threshold values of the three variables of interest, i.e. current speed, relative speed with

respect to the target-lane vehicles, and available gap in the target lane. The vehicle actually moves to its target lane only if three corresponding inequality conditions, involving the respective threshold values, are jointly satisfied.

In the microscopic simulation model, an on-ramp is followed by an acceleration lane, and the vehicles entering from the ramps need to change lane in order to eventually pass to the motorway mainstream. In these acceleration lanes, the default lane-changing model is replaced by the heuristic rules so as to achieve realistic driver merging. Similarly, the aforementioned rule-based approach is applied to the lane-drop region where the default model may result in unreasonably long queues on the dropping lane, that may persist until the end of the simulation. In conclusion, the lane-changing rules are applied at the critical on-ramp and lane-drop areas, while in the rest of the motorway, the Gipps lane-changing model is retained.

Besides the vehicle behavioral models, the dynamic demands scenario needs to be defined for the microscopic simulation assessment. The real data measurements retrieved from the field, consist of speed and flow measurements from several days during years 2009 and 2010. The dataset collected on "Wednesday 26-05-2010" is selected for model calibration, while other datasets are used to validate the calibrated model. The duration of the simulation is 4 hours, same as the real data measurements duration. Hence, the traffic demand assigned in the simulation scenario is composed of 240 values of one minute duration each. The simulation step of the microscopic traffic simulator, namely the intervals at which car-following and lane-changing rules are executed is set equal to 0.4 s.

3.3. Calibration of microscopic traffic simulation model

The reliability of the tests to be conducted within the microscopic simulation environment is fostered with the calibration of the model parameters so as to achieve simulation conditions close to reality. To this end, once the case study network described in Section 3.1 is cautiously modeled, and the dynamic demand scenario is created in the microscopic traffic simulator, a sensitivity analysis was conducted in order to define the model parameters that have the biggest impact on the simulation output. In this sense, the most significant parameters of Aimsun to be tuned were identified to be the maximum vehicle acceleration, comfortable deceleration, time headway, desired speed, maximum give-way time, and minimum distance. These parameters are common for each type of vehicle, while, to capture the stochastic behavior of individual drivers, a truncated normal distribution is used.

The calibration of those model parameters is a time consuming and challenging task, as they have to be calibrated simultaneously, taking into account the mutual correlation between the selected parameters. For best efficiency and convergence, the calibration procedure is formulated as an optimization problem, and a Genetic Algorithm (GA) is employed for its solution. GA has been widely applied for the calibration of microscopic simulation models (Cheu et al. 1998; Ma and Abdulhai 2002; Zhizhou et al. 2005; Park and Qi 2006) with parameter combination chromosomes that are evaluated based on an appropriately defined fitness function. The main advantage of the GA consists in searching for solutions at multiple points, instead of one single point, which typically leads to higher probability of finding a good local or even the global optimum (Kim and Rilett, 2001).

In the present work, the Root Mean Square Error (RMSE) between the simulated and the observed speeds is used as the objective function to be minimized, and the solution of the optimization problem delivers an optimal combination of values of the most influential model parameters. Moreover, it is ensured that the model parameters do not exceed any physical limits by constraining them within assigned lower and upper bounds. Note that, a calibration process that aims at achieving good fit between the model and reality using speed data instead of traffic volume is much more challenging, since any calibration outcome will satisfy the conservation-of-vehicles law and the simulated flow will eventually flow out. On the contrary, tuning the model parameters in order to match the speed dynamics on the motorway stretch is more challenging task.

Figure 4 illustrates the automated calibration procedure that aims at minimizing the objective function and finding a proper set of mean values for the simulation parameters of interest. The lower and upper bounds of the truncated normal distribution of each parameter are set based on the resulted mean value and a predefined standard deviation value. After the optimization-based parameter specification, the rest of the parameters of the traffic simulator, that have a lower influence on the simulation performance, are manually fine-tuned to achieve an even smaller RMSE value. Regarding the modified lane-changing model described in Section 3.2, the heuristic lane-changing rules were initially tuned in the acceleration lanes and the lane-drop region based on visual assessment of the resulting vehicle merging behavior; after the parameter calibration, they were re-tuned in the lane-drop section so as to reduce the discrepancies between the congestion length formed within

the microscopic simulation against the length appearing in reality.

The upper row of Figure 5 displays the speeds observed in the field, while in the lower row, the speeds produced by the microscopic simulation are displayed. The main objective of the calibration process in the present work was the tuning of the simulation model parameters so as to replicate the mainline congestion that starts at 06:20 a.m due to the increased demand at the on-ramp Nieuwerkerk a/d IJssel. Given that there was no interest in reproducing the traffic jams spilling back from the exit of the network[2], Figure 5 indicates that the microscopic simulation replicates reality with sufficient adequacy. Note that the data around the spillback congestion were excluded from the RMSE calculation for model calibration. The microscopic simulation model appropriately captures the onset of congestion, which is triggered by an increasing of demand at the first on-ramp (Nieuwerkerk a/d Ijssel). It is also observed that the starting time of congestion, duration and locations of the bottlenecks are in good agreement with reality. Finally, crucial traffic flow phenomena, like the capacity drop (see Figure 6), are successfully reproduced by the calibrated microscopic simulation model.

The calibrated model was further validated in order to confirm that it can replicate real traffic scenarios under other conditions as well. To this end, different demand profiles, reflecting real data collected from different days, were used, and it was concluded that the microscopic simulation can approach reality under other conditions as well. Table 1 includes the values

[2]Note that, if one wants to reproduce the traffic waves spilling back from downstream, appropriate boundary conditions need to be set for the simulator at the exit of the motorway.

of the RMSE between the real and the simulated speeds considering the data sets collected on different days. The seemingly high RMSE values stem from the fact that the error is evaluated on a lane-by-lane basis and with a sampling time of one minute for the entire simulation horizon which naturally increases the resulting RMSE as compared to cross-lane evaluations on bigger sampling times. Notwithstanding, the principal aim of the calibration process in the present work is to ensure that the utilized simulation model reflects adequately the challenging real traffic conditions and can therefore be used to demonstrate the difference between control and no-control results. More details regarding the validation process and results can be found in (Perraki, 2016).

4. Application and Results

4.1. MPC application

4.1.1. Optimization problem setup

For the MPC application, the benchmark network is subdivided in 21 segments with the length of each segment indicated in Figure 3. The same dicretization stands for the microscopic case study model which consists of 21 sections with identical features as the ones defined for the macroscopic model. Based on these lengths, the control step for the traffic flow model is set to $T = 10$ s, which is the maximum value that satisfies the stability condition CFL (Courant et al., 1928). A prediction horizon of 10 min is selected for the MPC problem, which is adequate to traverse the major part of the motorway stretch, so as to avoid myopic control actions. The control actions are updated and applied to the microscopic simulation model based

on the latest measurements and predictions every 1 min, which is deemed sufficient for real-time responsiveness as well as for the numerical solution of the optimization problem.

Fixed detectors at the motorway mainstream and at the on-ramp entrances are used to measure the flow entering the motorway. The demand during the rolling optimization horizon is predicted in a naive way, i.e. set constant during each prediction horizon and updated for the next optimization horizon based on the exponentially smoothed value that has been computed from the actual measured demand up to that point in time. The queue lengths at each on-ramp and the cell densities and speeds, which are used as initial conditions for each MPC optimization problem, are taken directly from the simulator. Clearly, in a real implementation, these values would be available from corresponding measurements or estimates.

In order to avoid an excessive constraining of the longitudinal flows within the optimization problem, a control step equal to the macroscopic model step is chosen for the MTFC actions as mentioned earlier. The optimal longitudinal flow values are subsequently averaged, based on the control application step which is 1 min, and converted to the respective VSL actions to be executed by VACS-equipped vehicles.

Since the proposed traffic flow model allows the introduction of different parameter values of the fundamental diagram for each cell, it was decided to use two different FDs. Considering that segment 8 contains the lane-drop, strong lateral movements are expected from lane 3 to lane 2. These intense lane-changing actions cause a drop of capacity in lane 2, which cannot accommodate equally high longitudinal flows as the other cells. Thus, a

fundamental diagram with lower capacity value is used for cell $(8, 2)$ and a different one for the rest of the network. Note that the possibility to account for a capacity reduction due to the lateral movements may be included in the optimization model. However, it was decided, for the sake of simplicity, to refrain from the exploitation of this option, since the capacity of the motorway seemed to remain unaffected by the lateral flow, except for the aforementioned cell.

The values of the fixed upper bounds for the on-ramp queues and flows $w_{i,j}^{max}$, $r_{i,j}^{max}$ and for the off-ramp flow $q_{i,j}^{off}$, as well as the values of the maximum lateral flows f^{max} were manually tuned based on the outcome of the MPC application in one single replication with the overall purpose of achieving a good match and performance in the microscopic simulation environment. The selected values were subsequently used to evaluate the performance of the MPC scheme in the rest of the replications. Additionally, the parameters of the two employed FDs have been identified based on the critical values (capacity flows ($q_{i,j}^{max}$), critical densities ($\rho_{i,j}^{cr}$), under-critical speeds (v^{free}) etc.) observed at each location of the stretch while running the specific replication and the cost weighting coefficients of the optimization problem have been specified taking into account the infrastructure features of the motorway. Specifically, a low-valued weight coefficient is set for the lateral flow penalization for segments 6,7, and 8 from lane 3 towards lane 2 in order to encourage the vehicles approaching the lane-drop to change lane in advance and thus mitigate potential bottlenecks in the region. Similarly, a low weight is chosen for the penalization of the lateral movements in segments 9 and 15, from lane 1 to lane 2 so as to prevent high densities in lane

1 due to the subsequent merging on-ramp.

The same dynamic scenario utilized for model calibration is used so as to test the efficiency of the MPC scheme under realistic conditions. Merely the time varying turning rates are replaced with the respective constant mean value for each off-ramp during the simulation period. The latter is necessary because, in case of time-varying turning rates, the control application would influence the exiting volumes from the off-ramps, and as a consequence, the total traveled distance. Hence, the TTS would not be comparable for the no-control versus control cases.

4.1.2. Implementation of the control strategy

During the control application, the speed of each equipped vehicle is computed based on the microscopic car-following rules, and is then bounded if it exceeds the VSL ordered by the controller for the respective cell. The speed of the manually driven vehicles is computed based on the local (fixed) speed limit value defined for each section of the microscopic model, similarly to the case that no control strategy is applied to the motorway.

For the LCC application, the optimal lateral flows derived from the optimization layer are translated to a respective number of lane-changing advises. These lane-changing commands are sent during the microscopic simulation to a number of selected equipped vehicles that are considered to result in the least negative impact on traffic flow after changing lane. In case no vehicles are capable to change lane as requested, the last command is repeated within the next simulation step(s). In the present application, it is considered that the drivers of the equipped vehicles that receive lane-changing demands are in full compliance with these advices, subject only to physical constraints

that may disallow a vehicle to actually change its lane. More specifically, while the lane-changing commands are sent to the selected vehicles during the simulation, the microscopic model's gap-acceptance and safety conditions need to be satisfied in order to attain the execution of the lane-change. However, any deviation between the optimal lateral flows and the actually executed lane changes may be partially compensated thanks to the feedback nature of the MPC. Note also that due to the implemented approach on the lane-changing execution, a minimum required time between two consecutive lane-change commands within the same cell is taken into account in order to avoid unrealistic number of lane-changes in very short intervals. Additionally, the vehicles that plan to exit from the motorway via off-ramps are excluded from the list of candidates to accomplish the optimal lateral flows and therefore their route remain unaffected from the control application. The manually driven cars, in case of mixed traffic conditions, as well as the VACS-equipped vehicles that do not receive orders to change lane, simply follow the maneuvers determined by the default lane-changing model employed in the microscopic simulation model. The control step for the LCC actions within the MPC is set equal to 1 min.

The RM control actions are independent from the presence of VACS-equipped vehicles in the motorway. Conventional traffic lights are placed about 10 m upstream of each on-ramp nose, with the intention of controlling the rate of vehicles entering the motorway. Appropriate green and red phases, are computed to implement the optimal ramp inflow resulted from the MPC for each control step, which is set to 1 min for RM as well.

4.2. Conducted experiments

The calibrated microscopic simulation model, as presented in Section 3.3, is capable of replicating reality with good accuracy. Although the tuning of the simulation model parameters was conducted using a single replication, in order to enhance the statistical significance of the assessments results, a set of 10 replications is used for each investigated scenario. For each of these replications, the same values resulted from the calibration process are utilized for the stochastic parameters, using however a different random seed for the generation of each vehicle's characteristics. Despite this change, all the no-control replications are reproducing the start time, the duration and the location of congestion similarly to the original employed replication illustrated in Figure 5.

In the next sections, the effectiveness of the MPC framework, is tested under different conditions and traffic control scenarios. Section 4.2.1 gives an overview of the traffic conditions in the motorway without the application of any control scheme. Then, in Section 4.2.2, the efficiency of the optimal control actions is examined for the cases of 100% VACS-equipped vehicle fleet, as well as for mixed traffic conditions. Section 4.2.3 assesses the efficiency of the control strategy in case conventional RM actions, which are not enabled by VACS, are disabled.

4.2.1. No-control case

The first experiment concerns the evaluation of the calibrated microscopic simulation model without the application of any control strategy. As described in Section 3.3, the traffic pattern of the microsimulation matches the real traffic conditions, i.e. the congestion is triggered at around 06:20 a.m.

due to the increased demand at an on-ramp and spreads further upstream, where the situation is deteriorated further due to the lane-drop. Eventually, the congestion dissolves at 08:00 am. This case is used as a reference case in order to assess the performance of the presented traffic management framework.

The strong congestion pattern is reproduced by the set of 10 replications, and the acquired average TTS in the motorway for the 4-hour simulation period, is TTS=1335 veh·h with a standard deviation of 89 veh·h. In the following experiments, the average results of the control application are presented, but the outcome of the replication with the closest TTS to the average value is more thoroughly described. Figure 7 shows the traffic situation for this replication in case no control actions are applied.

4.2.2. MPC under different penetration rates

In this section, the efficiency of the MPC strategy is examined for the cases of fully and partially VACS-equipped environments. It is considered that in the 100% penetration rate case, all vehicles are capable of sending information required for the optimization problem as well as receiving and executing control tasks. On the contrary, in the case of mixed traffic conditions, where the simulated flow consists of conventional and equipped vehicles, only a limited number of vehicles can implement the traffic control decisions.

In the latter case, only the vehicles equipped with VACS are receiving the VSL decided by the controller; whereas, for the remaining vehicles, the maximum speed is computed according to the nominal speed limit defined for the motorway, i.e. 120 km/h. Similarly, for the LCC, only vehicles equipped with intelligent devices are able to receive and implement lane-changing com-

mands. Therefore, in order to avoid strong discrepancies between the optimal lateral flow and the actually accomplished one due to insufficient amount of equipped vehicles, the upper bound of the lateral flow f^{max} is decreased proportionally to the penetration rate reduction. Finally, the introduction of mixed traffic conditions in the motorway does not affect the RM application, since traffic lights control the inflow from the on-ramps.

The MPC control scheme is evaluated under the assumption of 100%, 50% and 20% penetration rates, each with a set of 10 replications. The average results of the application are presented in Table 2. The overall improvement on the TTS value in the 100% penetration rate case is, as expected, the highest, compared to the lower penetration, with a reduction of 18.5 % in the average TTS and 77 % in TTS standard deviation. However, even for the cases of 50% and 20% of equipped vehicles, the control strategy leads to significant amelioration of the traffic conditions, since the average time spent is decreased by 17.4% and 13.9%, respectively. Note that the improvement on the TTS standard deviation values implies that the variation of traffic conditions from replication to replication is accordingly lower when the control scheme is applied. Hence, this improvement which is much more pronounced at high penetration rates, reflects increased travel time reliability which is a significant objective of modern traffic systems.

In order to examine in more detail how the controller manages to mitigate traffic congestion, some results of the replication with a TTS value closest to the average are presented. Figure 8 displays the speeds with MPC, for the cases of 100% (upper row) and 50% (lower row) penetration rates. In the case of a fully VACS-equipped traffic, it appears that the LCC and RM actions are

capable of avoiding traffic congestion without strong MTFC actions. On the other hand, the decrease of the penetration rate, and, as a consequence, of the possible maximum lateral flows, leads to the request of more intense MTFC actions from the optimizer in the 50% case. Thus, the small congestion appearing in the second row of Figure 8, is a consequence of the MTFC actions which aim to achieve capacity flow at the downstream bottleneck.

The improvement of the traffic conditions in the motorway stems mainly from the mitigation of the congestion-induced capacity drop, which leads to queue discharge rates lower than the free-flow capacity. Figure 9 indicates that, indeed, the throughput during the peak period is increased downstream of the bottleneck location, and the motorway operates at flow rates closer to its nominal capacity thanks to the applied control strategy. The performed integrated control actions, which result in this improvement are:

- Strong LCC actions are performed in segments 6, 7, and 8 in order to move vehicles from lane 3 to the adjacent lane before approaching the lane-drop location. In order to create sufficient space in lane 2 to accommodate the flow entering from lane 3, lateral movements are also requested from lane 2 to lane 1. Figure 10 displays the computed optimal lateral flows and the actually accomplished (within the microscopic simulation), right lateral movements for segment 7.

- The congestion due to the increased demand at the Nieuwerkerk aan den IJssel on-ramp is avoided with the application of RM at periods of high demand flow. At the same time, LCC actions are performed at the segment upstream the on-ramp i.e. segment 9, from lane 1 to

lane 2, allowing to maintain capacity flow (see Figure 9) and to avoid significant speed breakdown.

- The aforementioned LCC and RM actions, prevent the appearance of traffic congestion in the case of 100% equipped vehicles in the motorway. However, for partially automated traffic, the speed breakdown at the bottleneck is avoided via additional MTFC actions from 6:30 AM until 7:00 AM, which limit the flow arriving from upstream by the creation of the short-lived controlled congestion appearing in the lower row of Figure 8. Note, however, that the speed within this controlled congestion in lanes 2 and 3 has a higher value than the one in the no-control case. Figure 11 illustrates the speed limits that are requested from the MPC in the case of partially equipped environment in order to create a controlled congestion at segment 4 and the actual measured speeds at this location during the microscopic simulation.

- Left lateral movements are also requested in the segment upstream of the Moordrecht on-ramp in order to avoid traffic jams at that location. In parallel, RM actions are also applied in periods with high demand at this on-ramp.

4.2.3. MPC under different penetration rates without RM

The contribution of RM to the travel time reduction is tested with the application of the control framework considering only the integrated MTFC and LCC actions. The possibility of controlling the on-ramps is excluded within the optimization problem by setting an upper bound, w^{max}, equal

to 0 for the on-ramp queues while the traffic lights are deactivated in the microscopic simulation.

Table 3 contains the results of this scenario, examined again for the set of 10 replications and employing the same three the assumption of 3 different penetration rates. The average results of TTS reduction, compared to the no-control case, reveal that the application of the control scheme taking into account only the control actions executed by VACS is capable of mitigating traffic congestion efficiently. Specifically, for the 100% and 50% cases, the time spent in the motorway is decreased by 16.4% and 15.9%, respectively, which is only a small deterioration of less than 2.1% compared to the respective cases where RM is also integrated in the controller. However, for a lower penetration rate as 20%, where less vehicles are able to accomplish control tasks, the improvement is lower. In particular, in the conducted experiment without RM, the TTS is improved by 7.9%, which is a drop of 6% with respect to the original control application, while the standard deviation of the TTS is roughly equal to the no-control case.

Figure 12 illustrates the traffic conditions in the motorway, for the 100% and 50% penetration rates, with the modified MPC application. As expected, stronger MTFC actions are requested from the controller in both cases, due to the lack of flow control measures at the on-ramps. However, given that in the 50% case there is limited feasibility regarding the LCC actions, these MTFC actions are inevitably more intense compared to the 100% penetration rate case.

The results of this section emphasize the fact that conventional traffic control measures, such as RM, may have to be employed during the transition

period where only a minority of vehicles are equipped so as to receive and execute commands from a traffic management center. But even at high penetration of equipped vehicles, RM may be valuable in holding back traffic at the on-ramps and mitigating congestion at periods of high demand.

4.2.4. Statistical validity of results

Several studies have been carried out on the validity of microscopic traffic simulation models and the required simulation runs (see e.g. Toledo and Koutsopoulos 2004 and Truong et al. 2015). In the experiments illustrated here, the accuracy of the microscopic simulation model is ensured by the calibration process, that results in simulation performance close to reality for the no-control case. However, in order to further confirm the robustness of the presented traffic management framework, a statistical test was performed. Specifically, a paired sample t-test has been conducted in order to prove that the mean difference between the TTS in the performed replications in the no-control and in the control cases is significantly different from zero. The null hypothesis $H_0 : \mu = 0$ states that the improvement on the TTS due to the control application is due to random variation and the alternative hypothesis $H_A : \mu \neq 0$ declares that the mean difference between the no-control and the control cases is not equal to zero. Since the resulted p-value is < 0.02 for all the conducted control experiments the null hypothesis is rejected and we can imply that there is significant difference between the TTS in the no-control and in the control cases, at a 98% confidence interval.

5. Conclusions

The effectiveness of the MPC approach proposed by Roncoli et al. (2016a) has been tested for a realistic complex infrastructure using the microscopic traffic simulator Aimsun, which is initially calibrated in order to ensure the reliability of the simulation performance. The test site network is a stretch of the motorway A20 from Rotterdam to Gouda in the Netherlands with two couples of on-off/ramps, a lane-drop and a traffic pattern that leads to strong recurrent congestion. The application of the control strategy has been examined for the cases of fully VACS-equipped traffic and also for mixed traffic conditions, with conventional vehicles and various penetration rates of equipped vehicles. The outcome of this thorough investigation revealed that the integrated control actions are able to relieve or even utterly avoid the traffic congestion in the motorway under high and lower penetration rates. A second traffic control scenario has been employed in order to assess the impact of the conventional RM action by removing them from the integrated traffic control problem. The obtained results indicate that the control actions executed by VACS-equipped vehicles have the potential to mitigate traffic congestion even without the use of conventional control measures, since especially for high penetration rates the difference between the improvement on the TTS is rather small for the two scenarios. On the other hand, for lower penetration rates or higher demands, the achieved improvements may be reduced, and this underlines the usefulness of conventional traffic control measures, such as RM, during the transition period, but also in a fully equipped traffic environment where demands may be increased compared to the current levels.

Acknowledgements

The research leading to these results has been conducted in the frame of the project TRAMAN21, which has received funding from the European Research Council under the European Union's Seventh Framework Programme (FP/2007-2013)/ERC Advanced Grant Agreement n. 321132.
The authors would like to thank Prof. Bart van Arem and his group for their support in providing information related to the network used in the application example.

References

Abdel-Aty, M. A., Dhindsa, A., 2007. Coordinated use of variable speed limits and ramp metering for improving safety on congested freeways. In: Transportation Research Board 86th Annual Meeting.

Ammoun, S., Nashashibi, F., Laurgeau, C., 2007. An analysis of the lane changing manoeuvre on roads: the contribution of inter-vehicle cooperation via communication. In: IEEE Conference on Intelligent Vehicles Symposium. pp. 1095–1100.

Baskar, L. D., De Schutter, B., Hellendoorn, J., Papp, Z., 2011. Traffic control and intelligent vehicle highway systems: a survey. IET Intelligent Transport Systems 5 (1), 38–52.

Baskar, L. D., Schutter, B. D., Hellendoorn, H., 2012. Traffic management for automated highway systems using model-based predictive control. IEEE Transactions on Intelligent Transportation Systems 13 (2), 838–847.

Bekiaris-Liberis, N., Roncoli, C., Papageorgiou, M., 2016. Highway traffic state estimation with mixed connected and conventional vehicles. IEEE Transactions on Intelligent Transportation Systems 17 (12), 3484–3497.

Bekiaris-Liberis, N., Roncoli, C., Papageorgiou, M., 2017. Highway traffic state estimation per lane in the presence of connected vehicles. Transportation Research Part B: Methodological 106, 1–28.

Breton, P., Hegyi, A., De Schutter, B., Hellendoorn, H., 2002. Shock wave elimination/reduction by optimal coordination of variable speed limits. In: IEEE Conference on Intelligent Transportation Systems. pp. 225–230.

Carlson, R. C., Papamichail, I., Papageorgiou, M., 2011. Local feedback-based mainstream traffic flow control on motorways using variable speed limits. IEEE Transactions on Intelligent Transportation Systems 12 (4), 1261–1276.

Carlson, R. C., Papamichail, I., Papageorgiou, M., Messmer, A., 2010. Optimal motorway traffic flow control involving variable speed limits and ramp metering. Transportation Science 44 (2), 238–253.

Cheu, R.-L., Jin, X., Ng, K.-C., Ng, Y.-L., Srinivasan, D., 1998. Calibration of fresim for singapore expressway using genetic algorithm. Journal of Transportation Engineering 124 (6), 526–535.

Chevallier, E., Leclercq, L., 2009. Do microscopic merging models reproduce the observed priority sharing ratio in congestion? Transportation Research Part C: Emerging Technologies 17 (3), 328–336.

Courant, R., Friedrichs, K., Lewy, H., 1928. Über die partiellen differenzengleichungen der mathematischen physik. Mathematische annalen 100 (1), 32–74.

Daganzo, C. F., 1994. The cell transmission model: A dynamic representation of highway traffic consistent with the hydrodynamic theory. Transportation Research Part B: Methodological 28 (4), 269–287.

Dao, T.-S., Clark, C. M., Huissoon, J. P., 2007. Optimized lane assignment using inter-vehicle communication. In: IEEE Conference on Intelligent Vehicles Symposium. pp. 1217–1222.

Dao, T.-S., Clark, C. M., Huissoon, J. P., 2008. Distributed platoon assignment and lane selection for traffic flow optimization. In: IEEE Conference on Intelligent Vehicles Symposium. pp. 739–744.

Davarynejad, M., Hegyi, A., Vrancken, J., van den Berg, J., 2011. Motorway ramp-metering control with queuing consideration using q-learning. In: IEEE Conference on Intelligent Transportation Systems. pp. 1652–1658.

Davis, L., 2004. Effect of adaptive cruise control systems on traffic flow. Physical Review E 69 (6), 66–110.

Diakaki, C., Papageorgiou, M., Papamichail, I., Nikolos, I., 2015. Overview and analysis of vehicle automation and communication systems from a motorway traffic management perspective. Transportation Research Part A: Policy and Practice 75, 147–165.

Fountoulakis, M., Bekiaris-Liberis, N., Roncoli, C., Papamichail, I., Papageorgiou, M., 2017. Highway traffic state estimation with mixed connected

and conventional vehicles: Microscopic simulation-based testing. Transportation Research Part C: Emerging Technologies 78, 13–33.

Gipps, P., 1981. A behavioural car-following model for computer simulation. Transportation Research Part B: Methodological 15 (2), 105–111.

Gipps, P., 1986. A model for the structure of lane-changing decisions. Transportation Research Part B: Methodological 20 (5), 403–414.

Hegyi, A., De Schutter, B., Hellendoorn, H., 2005a. Model predictive control for optimal coordination of ramp metering and variable speed limits. Transportation Research Part C: Emerging Technologies 13 (3), 185–209.

Hegyi, A., De Schutter, B., Hellendoorn, J., 2005b. Optimal coordination of variable speed limits to suppress shock waves. IEEE Transactions on intelligent transportation systems 6 (1), 102–112.

Iordanidou, G.-R., Papamichail, I., Roncoli, C., Papageorgiou, M., 2017. Feedback-based integrated motorway traffic flow control with delay balancing. IEEE Transactions on Intelligent Transportation Systems 18 (9), 2319–2329.

Iordanidou, G.-R., Roncoli, C., Papamichail, I., Papageorgiou, M., 2015. Feedback-based mainstream traffic flow control for multiple bottlenecks on motorways. IEEE Transactions on Intelligent Transportation Systems 16 (2), 610–621.

Kesting, A., Treiber, M., Helbing, D., 2010. Enhanced intelligent driver model to access the impact of driving strategies on traffic capacity. Philo-

sophical Transactions of the Royal Society A: Mathematical, Physical and Engineering Sciences 368 (1928), 4585–4605.

Kesting, A., Treiber, M., Schönhof, M., Helbing, D., 2007. Extending adaptive cruise control to adaptive driving strategies. Transportation Research Record: Journal of the Transportation Research Board (2000), 16–24.

Kim, K., Medanić, J. V., Cho, D. I., 2008. Lane assignment problem using a genetic algorithm in the automated highway systems. International Journal of Automotive Technology 9 (3), 353–364.

Kim, K.-O., Rilett, L., 2001. Genetic-algorithm based approach for calibrating microscopic simulation models. In: IEEE Conference on Intelligent Transportation Systems. pp. 698–704.

Kontorinaki, M., Spiliopoulou, A., Roncoli, C., Papageorgiou, M., 2017. First-order traffic flow models incorporating capacity drop: Overview and real-data validation. Transportation Research Part B: Methodological 106, 52–75.

Kotsialos, A., Papageorgiou, M., 2004. Nonlinear optimal control applied to coordinated ramp metering. IEEE Transactions on control systems technology 12 (6), 920–933.

Kotsialos, A., Papageorgiou, M., Mangeas, M., Haj-Salem, H., 2002. Coordinated and integrated control of motorway networks via non-linear optimal control. Transportation Research Part C: Emerging Technologies 10 (1), 65–84.

Lee, C., Hellinga, B., Saccomanno, F., 2006. Evaluation of variable speed limits to improve traffic safety. Transportation research part C: Emerging Technologies 14 (3), 213–228.

Lighthill, M. J., Whitham, G. B., 1955. On kinematic waves. ii. a theory of traffic flow on long crowded roads. In: Proceedings of the Royal Society of London A: Mathematical, Physical and Engineering Sciences. Vol. 229. pp. 317–345.

Ma, T., Abdulhai, B., 2002. Genetic algorithm-based optimization approach and generic tool for calibrating traffic microscopic simulation parameters. Transportation Research Record: Journal of the Transportation Research Board (1800), 6–15.

Milanés, V., Shladover, S. E., 2014. Modeling cooperative and autonomous adaptive cruise control dynamic responses using experimental data. Transportation Research Part C: Emerging Technologies 48, 285–300.

Nie, J., Zhang, J., Ding, W., Wan, X., Chen, X., Ran, B., 2016. Decentralized cooperative lane-changing decision-making for connected autonomous vehicles. IEEE Access 4, 9413–9420.

Papadopoulou, S., Roncoli, C., Bekiaris-Liberis, N., Papamichail, I., Papageorgiou, M., 2018. Microscopic simulation-based validation of a per-lane traffic state estimation scheme for highways with connected vehicles. Transportation Research Part C: Emerging Technologies 86, 441–452.

Papageorgiou, M., 1984. Multilayer control system design applied to freeway traffic. IEEE transactions on automatic control 29 (6), 482–490.

Papageorgiou, M., Papamichail, I., 2008. Overview of traffic signal operation policies for ramp metering. Transportation Research Record: Journal of the transportation research board (2047), 28–36.

Papamichail, I., Kampitaki, K., Papageorgiou, M., Messmer, A., 2008. Integrated ramp metering and variable speed limit control of motorway traffic flow. IFAC Proceedings Volumes 41 (2), 14084–14089.

Papamichail, I., Kotsialos, A., Margonis, I., Papageorgiou, M., 2010. Coordinated ramp metering for freeway networks–a model-predictive hierarchical control approach. Transportation Research Part C: Emerging Technologies 18 (3), 311–331.

Park, B., Qi, H., 2006. Microscopic simulation model calibration and validation for freeway work zone network-a case study of vissim. In: IEEE Conference on Intelligent Transportation Systems. pp. 1471–1476.

Perraki, G., 2016. Evaluation of a model predictive control strategy on a calibrated multilane microscopic model. Master's thesis, School of Production Engineering and Management, Technical University of Crete.

Perraki, G., Roncoli, C., Papamichail, I., Papageorgiou, M., 2017. Evaluation of an MPC strategy for motorway traffic comprising connected and automated vehicles. In: IEEE Conference on Intelligent Transportation Systems. pp. 2315–2321.

Rao, B., Varaiya, P., 1993. Flow benefits of autonomous intelligent cruise control in mixed manual and automated traffic. Transportation Research Record: Journal of the Transportation Research Board (1408), 36–43.

Rao, B., Varaiya, P., 1994. Roadside intelligence for flow control in an intelligent vehicle and highway system. Transportation Research Part C: Emerging Technologies 2 (1), 49–72.

Roncoli, C., Papamichail, I., Papageorgiou, M., 2016a. Hierarchical model predictive control for multi-lane motorways in presence of vehicle automation and communication systems. Transportation Research Part C: Emerging Technologies 62, 117–132.

Roncoli, C., Bekiaris Liberis, N., Papageorgiou, M., 2016b. Optimal lane-changing control at motorway bottlenecks. In: IEEE Conference on Intelligent Transportation Systems. pp. 1785–1791.

Roncoli, C., Bekiaris-Liberis, N., Papageorgiou, M., 2017. Lane-changing feedback control for efficient lane assignment at motorway bottlenecks. Transportation Research Record: Journal of the Transportation Research Board (2625), 20–31.

Roncoli, C., Papageorgiou, M., Papamichail, I., 2015a. Traffic flow optimisation in presence of vehicle automation and communication systems – Part I: A first-order multi-lane model for motorway traffic. Transportation Research Part C: Emerging Technologies 57, 241–259.

Roncoli, C., Papageorgiou, M., Papamichail, I., 2015b. Traffic flow optimisation in presence of vehicle automation and communication systems – Part II: Optimal control for multi-lane motorways. Transportation Research Part C: Emerging Technologies 57, 260–275.

Schakel, W. J., van Arem, B., 2014. Improving traffic flow efficiency by in-car advice on lane, speed, and headway. IEEE Transactions on Intelligent Transportation Systems 15 (4), 1597–1606.

Shladover, S., Su, D., Lu, X.-Y., 2012. Impacts of cooperative adaptive cruise control on freeway traffic flow. Transportation Research Record: Journal of the Transportation Research Board (2324), 63–70.

Spiliopoulou, A., Perraki, G., Papageorgiou, M., Roncoli, C., 2017. Exploitation of ACC systems towards improved traffic flow efficiency. In: IEEE Conference on Models and Technologies for Intelligent Transportation Systems. pp. 37–43.

Toledo, T., Koutsopoulos, H. N., 2004. Statistical validation of traffic simulation models. Transportation Research Record: Journal of the Transportation Research Board (1876), 142–150.

Transport Simulation Systems, 2014. Aimsun 8 Dynamic Simulators Users' Manual. Transport Simulation Systems.

Treiber, M., Hennecke, A., Helbing, D., 2000. Congested traffic states in empirical observations and microscopic simulations. Physical Review E 62 (2), 1805–1824.

Truong, L. T., Sarvi, M., Currie, G., Garoni, T. M., 2015. Required traffic micro-simulation runs for reliable multivariate performance estimates. Journal of Advanced Transportation, 296–314.

van den Berg, M., Hegyi, A., De Schutter, B., Hellendoorn, J., 2007. Integrated traffic control for mixed urban and freeway networks: A model

predictive control approach. European journal of transport and infrastructure research 7 (3), 223–250.

Vander Werf, J., Shladover, S., Miller, M., Kourjanskaia, N., 2002. Effects of adaptive cruise control systems on highway traffic flow capacity. Transportation Research Record: Journal of the Transportation Research Board (1800), 78–84.

Varaiya, P., 1993. Smart cars on smart roads: problems of control. IEEE Transactions on Automatic Control 38 (2), 195–207.

Wang, J., Liu, R., Montgomery, F., 2005. Car-following model for motorway traffic. Transportation Research Record: Journal of the Transportation Research Board 1934, 33–42.

Wang, M., Daamen, W., Hoogendoorn, S. P., van Arem, B., 2014a. Rolling horizon control framework for driver assistance systems. – Part I: Mathematical formulation and non-cooperative systems. Transportation research part C: Emerging Technologies 40, 271–289.

Wang, M., Daamen, W., Hoogendoorn, S. P., van Arem, B., 2014b. Rolling horizon control framework for driver assistance systems. – Part II: Cooperative sensing and cooperative control. Transportation research part C: Emerging Technologies 40, 290–311.

Wang, M., Daamen, W., Hoogendoorn, S. P., Van Arem, B., 2016. Connected variable speed limits control and car-following control with vehicle-infrastructure communication to resolve stop-and-go waves. Journal of Intelligent Transportation Systems (6), 559–572.

Yang, X., Lin, Y., Lu, Y., Zou, N., 2013. Optimal variable speed limit control for real-time freeway congestions. Procedia-Social and Behavioral Sciences 96, 2362–2372.

Zhizhou, W., Jian, S., Xiaoguang, Y., 2005. Calibration of vissim for shanghai expressway using genetic algorithm. In: Simulation Conference, 2005 Proceedings of the Winter. pp. 2645–2648.

List of Figures

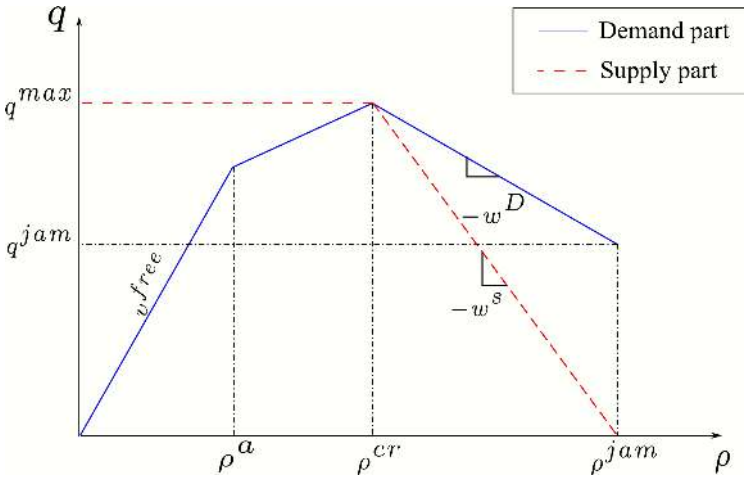

Figure 1: The proposed FD including both the demand (solid lines) and the supply (dashed lines) piecewise-linear functions.

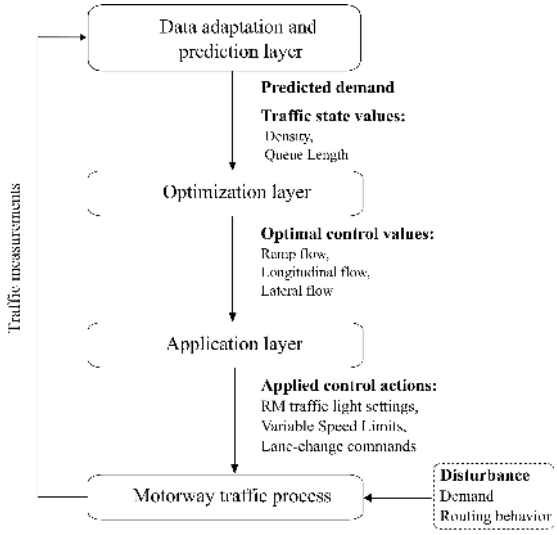

Figure 2: Multilayer control structure.

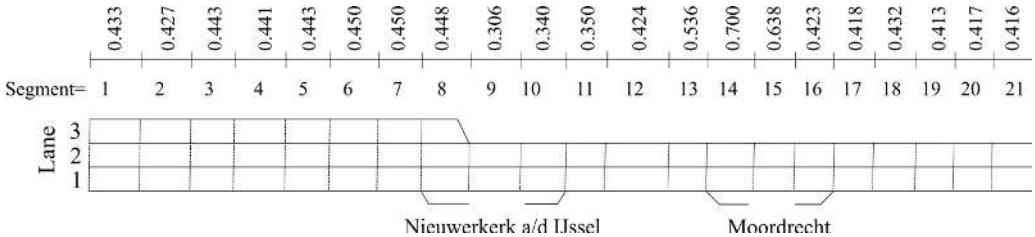

Figure 3: Stretch of the motorway A20 used as the case study network.

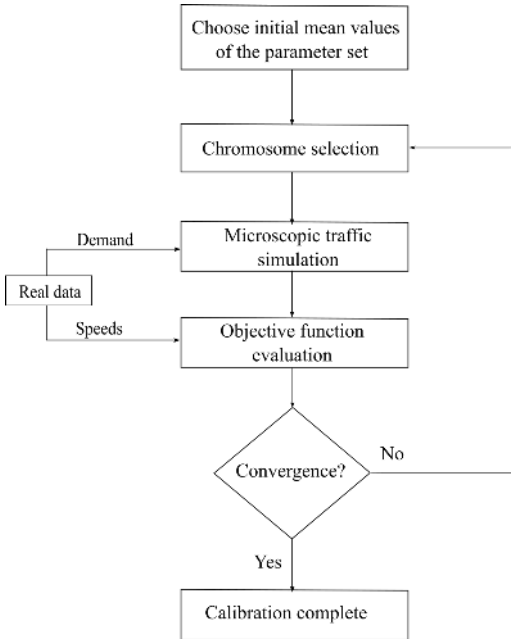

Figure 4: Optimization-based calibration process

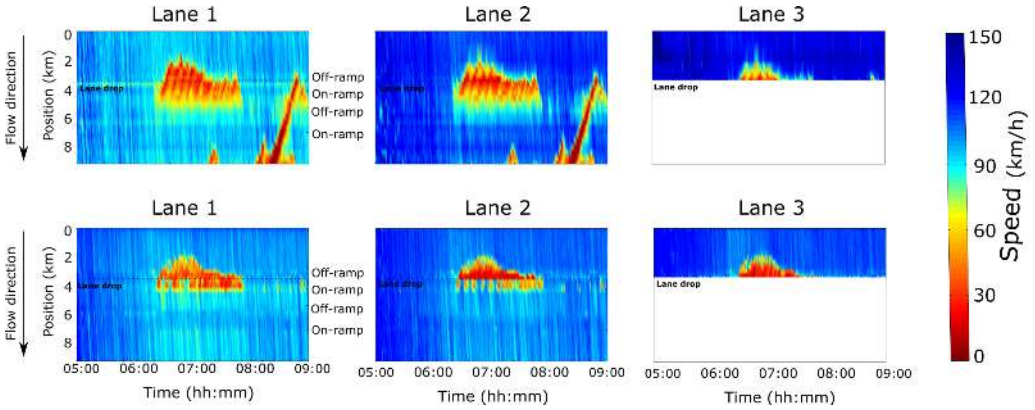

Figure 5: Contour plots for speeds observed in the field (upper row) and produced by the microscopic simulation (lower row).

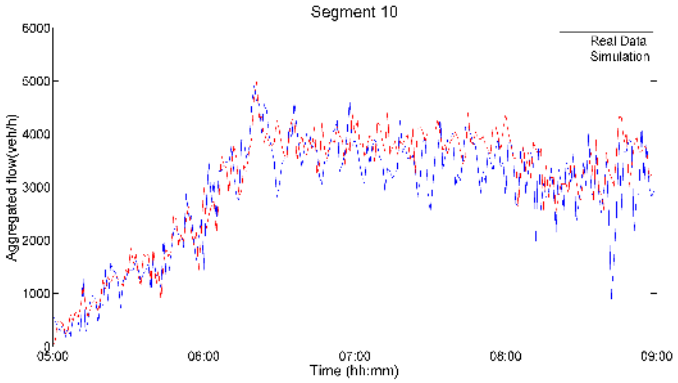

Figure 6: Aggregated flow exiting segment 10 reflecting the capacity drop reproduced by the traffic simulation model at the bottleneck location in a similar way as in real traffic.

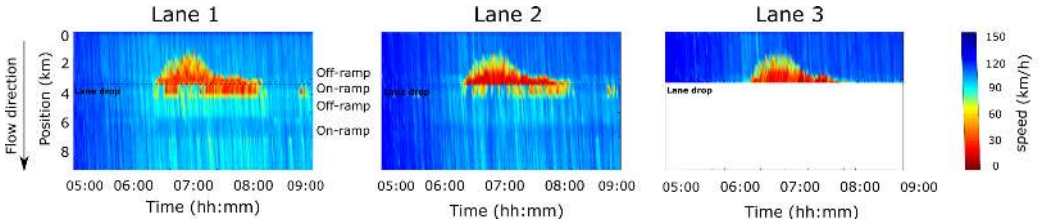

Figure 7: Contour plot for speeds in the no-control case for one replication.

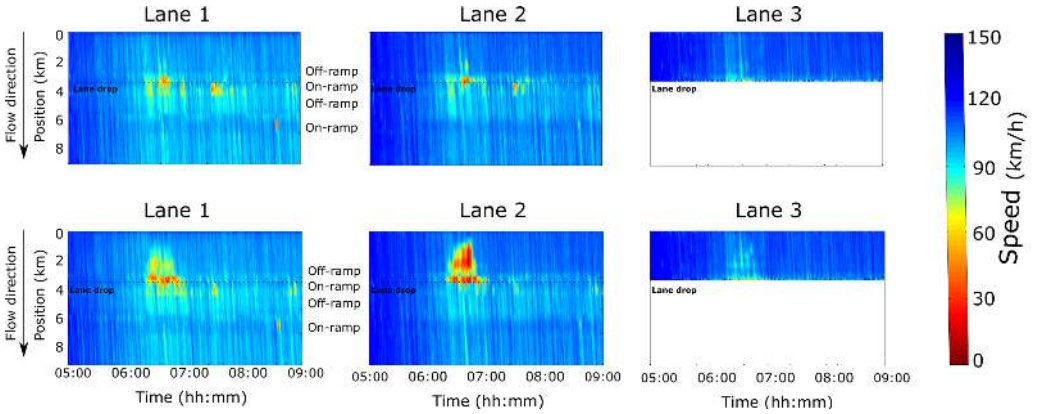

Figure 8: Contour plots for speeds in the control case, for 100% (upper row) and 50% penetration rate (lower row)

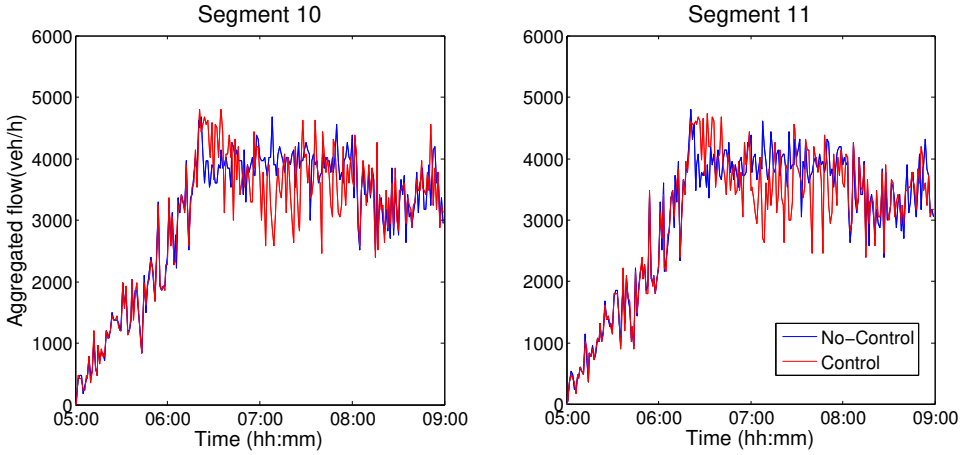

Figure 9: Comparison between aggregate flows in no-control (blue) and in the control (red) case with 100% penetration rate, at segments 10-11.

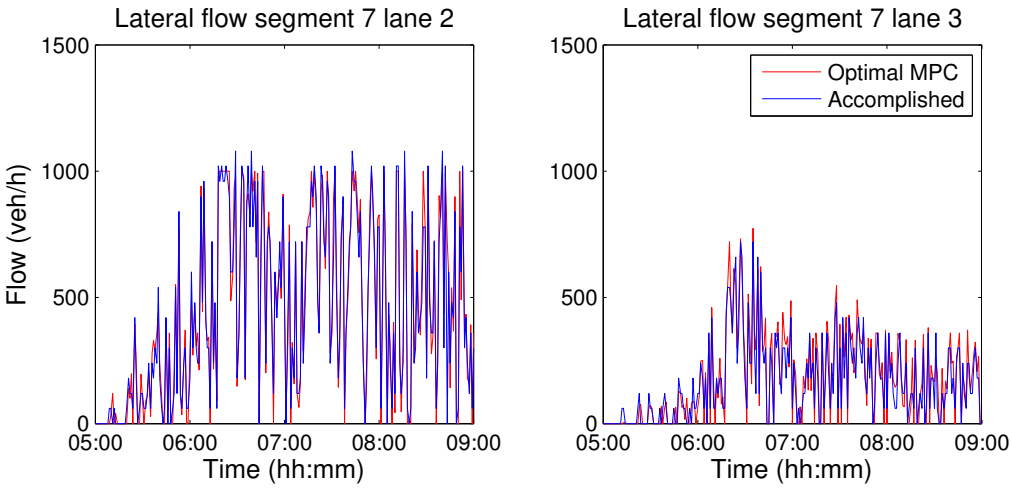

Figure 10: Comparison between optimal (red) and accomplished (blue) right lateral flows at segment 7 for 100% penetration rate.

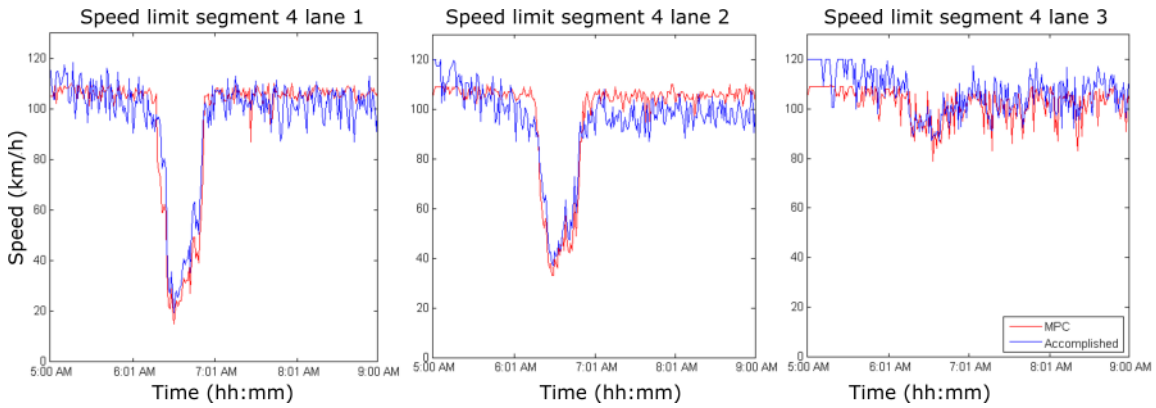

Figure 11: Comparison between optimal (red) and accomplished (blue) speed limits at segment 4 for 50% penetration rate.

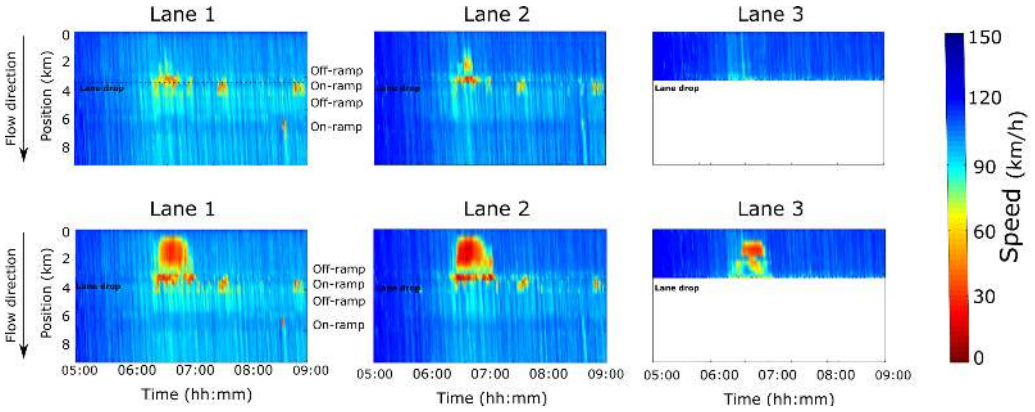

Figure 12: Contour plots for speeds in the control case without RM for 100% (upper row) and 50% penetration rate (lower row).

List of Tables

Table 1: RMSE between real and simulated speeds for the calibrated and the validated scenarios.

	Calibration	Validation		
Date	Wednesday, 26-05-2010	Monday, 08-06-2009	Thursday, 25-06-2009	Monday, 21-06-2010
RMSE (km/h)	17	17	14	19

Table 2: Average results of 10 replications for the MPC application

Penetration rate (%)	**TTS [veh·h]**		**TTS improvement (%)**	
	Average	S.D.	Average	S.D.
100	1088.5	20.5	18.5	77.0
50	1102.0	27.1	17.4	69.6
20	1149.7	69.5	13.9	22.1
No-Control case	1335.0	89.17	-	-

Table 3: Average results of 10 replications for the MPC application without RM

Penetration rate (%)	**TTS [veh·h]**		**TTS improvement (%)**	
	Average	S.D.	Average	S.D.
100	1116.4	30.9	16.4	65.4
50	1123.0	41.8	15.9	53.1
20	1229.2	88.2	7.9	1.1
No-Control case	1335.0	89.17	-	-